JPn Neuroscience

The Journal of Physiology

J Physiol 592.4 (2014) pp 557–569

RAPID REPORT

Subunit-specific inhibition of acid sensing ion channels by stomatin-like protein 1

Alexey Kozlenkov[1,3], Liudmila Lapatsina[1], Gary R. Lewin[1] and Ewan St. John Smith[1,2]

[1] *Department of Neuroscience, Max-Delbrück Center for Molecular Medicine, Robert-Rössle-Strasse 10, 13125 Berlin-Buch, Germany*
[2] *Department of Pharmacology, University of Cambridge, Tennis Court Road, Cambridge CB2 1PD, UK*
[3] *Current address: Department of Psychiatry, Mount Sinai School of Medicine, New York, New York, USA*

Key points

- Stomatin-like protein 1 (STOML1) was found both at the plasma membrane and associated with vesicles in the neurites of dorsal root ganglia (DRG) neurones.
- We found that STOML1 modulates ASIC1a and ASIC3. In the presence of STOML1 acid gated currents carried by ASIC1a were decreased and ASIC3 currents showed accelerated inactivation; STOML1 had no effects on other ASICs.
- Among the stomatin family, only STOML1 has a sterol carrier protein-2 domain and removal of this domain prevented inhibition of ASIC1a currents.
- We generated a mouse with a β-galactosidase-neomycin cassette gene-trap reporter driven from the STOML1 gene locus to demonstrate that STOML1 is expressed by approximately half of all DRG neurones.
- Whole-cell electrophysiology recordings from DRG neurones from *STOML1* null mutant mice showed on average larger proton-gated currents compared to neurones from wild-type mice.

Abstract There are five mammalian stomatin-domain genes, all of which encode peripheral membrane proteins that can modulate ion channel function. Here we examined the ability of stomatin-like protein 1 (STOML1) to modulate the proton-sensitive members of the acid-sensing ion channel (ASIC) family. STOML1 profoundly inhibits ASIC1a, but has no effect on the splice variant ASIC1b. The inactivation time constant of ASIC3 is also accelerated by STOML1. We examined STOML1 null mutant mice with a β-galactosidase-neomycin cassette gene-trap reporter driven from the STOML1 gene locus, which indicated that STOML1 is expressed in at least 50% of dorsal root ganglion (DRG) neurones. Patch clamp recordings from mouse DRG neurones identified a trend for larger proton-gated currents in neurones lacking STOML1, which was due to a contribution of effects upon both transient and sustained currents, at different pH, a finding consistent with an endogenous inhibitory function for STOML1.

(Received 10 May 2013; accepted after revision 16 November 2013; first published online 18 November 2013)
Corresponding author E. S. J. Smith or G. R. Lewin: Department of Neuroscience, Growth Factor & Regeneration Group, Max-Delbrueck Center for Molecular Medicine, Robert-Roessle Strasse 10, D-13092 Berlin, Germany. Email: es336@cam.ac.uk or glewin@mdc-berlin.de

Abbreviations ASIC, acid-sensing ion channel; CHO, Chinese hamster ovary; DRG, dorsal root ganglion; (E)GFP, (enhanced) green fluorescent protein; S current, sustained current; SCP2, sterol carrier protein-2; STOML-1, stomatin-like protein-1; T current, transient current; TRPV1, transient receptor potential vanilloid 1; X-gal, 5-bromo-4-chloro-3-indolyl-β-D-galactopyranoside.

DOI: 10.1113/jphysiol.2013.258657

Introduction

Proteins of the stomatin family are characterised by an evolutionarily conserved core domain called the stomatin domain (Tavernarakis *et al.* 1999; Lapatsina *et al.* 2012*a*). Due to the similarity of the stomatin domain to a domain found in the prohibitin, flotillin and HflK/HflC families, the stomatin-domain has also been called the SPFH domain. In mammals, the stomatin family consists of: stomatin, podicin and stomatin-like proteins 1–3 (STOML1, STOML2 and STOML3). Typically, stomatin domain-containing proteins are integral membrane proteins with a single membrane insertion domain and intracellular N and C termini; differences within the non-conserved C and N termini may underlie functional diversity of stomatin domain proteins. The crystal structure of the archaeobacterial stomatin core domain from *Pyrococcus horikoshii* showed that this stomatin domain can form trimeric homooligomers (Yokoyama *et al.* 2008). However, our X ray crystallographic and function studies on the mouse stomatin domain from stomatin indicated that this protein forms dimers (Brand *et al.* 2012).

Stomatin appears to be a ubiquitously expressed membrane protein that is absent from the plasma membrane of red blood cells in hereditary hydrocytosis, a haemolytic anaemia that is characterised by abnormal erythrocyte permeability to Na^+ and K^+, and this led to the hypothesis that stomatin may modulate ion channel and/or transporter function (Stewart *et al.* 1992; Gallagher & Forget, 1995). The strongest evidence for ion channel modulation by stomatin is the inhibitory role that different members of the stomatin family have upon specific subunits of the acid-sensing ion channel (ASIC) family, which are part of the Deg/ENaC superfamily. In mammals, four different genes encode six different ASIC subunits (ASIC1a/1b, ASIC2a/b, ASIC3 and ASIC4) that form both homomers and heteromers (Kellenberger & Schild, 2002; Sherwood *et al.* 2012). With the exception of homomeric ASIC2b and ASIC4, mammalian ASICs are activated by extracellular protons and there is evidence to suggest that ASIC-mediated acid sensing is involved peripherally to produce pain (Cadiou *et al.* 2007; Deval *et al.* 2008); the use of subunit-specific toxins combined with siRNA knockdown has also demonstrated important functions for both peripheral and spinal cord ASIC expression (Mazzuca *et al.* 2007; Diochot *et al.* 2012). In the central nervous system, ASICs have been demonstrated to have further roles in mediating ischaemic damage (Xiong *et al.* 2004), fear (Ziemann *et al.* 2009), epilepsy (Ziemann *et al.* 2008) and learning (Wemmie *et al.* 2002); ASIC1a is frequently described as being the key acid sensor centrally (Wemmie *et al.* 2013).

To date, it has been shown that stomatin inhibits ASIC3-mediated currents and accelerates the ASIC2a inactivation time constant (Price *et al.* 2004), effects that are absent in dimerisation-deficient stomatin mutant proteins (Brand *et al.* 2012). STOML3 has been shown to inhibit both ASIC2a- and ASIC3-mediated currents (Lapatsina *et al.* 2012*b*), which correlates with the significantly larger proton-gated currents observed in neurones from mice lacking STOML3 when compared to those from wild-type littermates (Wetzel *et al.* 2007). In addition to acid sensing, mechanosensory deficits have also been recorded in mice lacking ASICs (Price *et al.* 2000, 2001; Page *et al.* 2004; Jones *et al.* 2005). Similarly, evidence shows that members of the stomatin family are involved in mechanosensation across phyla (Smith & Lewin, 2009): 40% of skin mechanoreceptors in STOML3$^{-/-}$ mice are mechanically insensitive and mice display decreased tactile acuity (Wetzel *et al.* 2007); stomatin$^{-/-}$ mice also show deficits in mechanoreceptor function (Martinez-Salgado *et al.* 2007) and double mutants of stomatin domain proteins with ASIC2 or ASIC3 suggest that such interaction may modulate mechanosensory phenotypes (Moshourab *et al.* 2013). The stomatin orthologue MEC-2 is an essential component of a multiprotein, mechanotransduction complex in *Caenorhabditis elegans* (Goodman *et al.* 2002), a complex that also contains the ASIC-related, pore-forming ion channels MEC-4 and MEC-10 (O'Hagan *et al.* 2005). Stomatin has also been shown to inhibit pannexin-1 (Zhan *et al.* 2012), depress glucose transporter-1 activity (Zhang *et al.* 2001) and interact with several other erythrocyte membrane proteins (Rungaldier *et al.* 2013).

STOML1 is the least studied mammalian stomatin and has a C-terminal sterol carrier protein-2 (SCP2) domain that is absent from other mammalian stomatins. However, like STOML1, the *C. elegans* protein UNC-24 contains both a stomatin-like domain and an SCP2 domain (Barnes *et al.* 1996). Human STOML1 was cloned from brain tissue and is predominantly expressed in the nervous system (Seidel & Prohaska, 1998), but its function in mammals has remained largely unstudied. In cell lines it has been shown to localise to late endosomes and interact with stomatin, influencing its localisation (Mairhofer *et al.* 2009).

In this study, we have examined the ability of STOML1 to modulate ASICs using whole-cell electrophysiology and observed an inhibitory effect upon ASIC1a that is dependent upon the SCP2 domain. We also examined STOML1 null mutant mice and found evidence that native proton-gated currents are of larger magnitude in subsets of sensory neurones lacking STOML1 compared to wild-type controls.

Methods

STOML1 mutant mice

We used the gene-trap ES clone M038E05 from German Gene Trap Consortium (www.genetrap.org) to generate the STOML1 knockout mouse line, in which a betaGeo

gene-trap cassette (coding for a fusion protein of β-galactosidase and neomycin resistance enzyme) was inserted in place of the first exon of the STOML1 gene under the control of the STOML1 promoter. After blastocyst injection, and foster mother implantation of the ES clone, five chimeric F0 males were obtained, one of which produced F1 pups; three of the F1 pups were confirmed by PCR and Southern blotting to carry the mutant allele. The STOML1$^{+/-}$ mice were then back-crossed onto a C57BL/6 background for at least five generations. Animals both heterozygous and homozygous for the *STOML1* mutant allele were viable and displayed no overt neurological phenotypes. The complete absence of *STOML1* mRNA expression in the STOML1$^{-/-}$ animals was confirmed by quantitative PCR (data not shown).

Dorsal root ganglion (DRG) neurone cultures and transfection

All animal protocols were approved by the German federal authorities (State of Berlin). Adult C57BL/6 and transgenic STOML1$^{-/-}$ mice were killed by carbon dioxide inhalation. DRGs were isolated from all spinal levels and collected in Ca^{2+}-/Mg^{2+}-free PBS. DRGs were subsequently incubated in collagenase IV (1 mg ml^{-1}, 30 min, 37°C, Sigma-Aldrich, St Louis, MO, USA), followed by trypsin (0.05%, 25 min, 37°C, Invitrogen, Carlsbad, CA, USA). DRGs were washed twice with DRG growth medium [DMEM (Life Technologies GmbH, Darmstadt, Germany) containing 10% heat-inactivated horse serum (Biochrom, Cambridge, UK), 20 mM glutamine, 0.8% glucose, 100 U penicillin and 100 mg ml^{-1} streptomycin (Life Technologies)] and then triturated using 20G (×10) and 23G (×5) needles. Dissociated neurones were plated on to poly-L-lysine (200 mg ml^{-1}) and laminin (20 μg ml^{-1}) coated glass coverslips and kept at 37°C in 5% CO_2. For transfection, freshly prepared DRG neurones were transfected using the Nucleofector system (Amaxa Biosystems, Cologne, Germany). In brief, neurones from one animal were resuspended in 100 ml of Rat Neuron Nucleofector Solution and a total 4–7 mg of plasmid DNA at room temperature. The mixture was transferred to a cuvette and electroporated with the pre-installed programme A-033. After electroporation, cells were transferred to 1 ml of RPMI medium and plated on laminin-covered dishes or coverslips. All immunocytochemistry and live-cell imaging were conducted on cells 24–30 h after transfection.

CHO cell line transfection

Chinese hamster ovary (CHO) cells (European Collection of Cell Cultures) were cultured in F-12 Ham medium + L-glutamine (Gibco, Carlsbad, CA, USA) with 10% fetal calf serum (PAA) and 1% penicillin/streptomycin. Cells were plated on to poly-L-lysine coated 35 mm (TPP) dishes prior to transfection. Transfections were conducted with lipofectamine LTX (Invitrogen) according to the manufacturer's protocol. Plasmids of interest were transfected at a ratio of 1:1:0.1 [STOML1/ASICx/green fluorescent protein (GFP)], with a DNA concentration of 2 μg per 40 mm dish. All ASICs were from rat and STOML1 was from mouse; different constructs were used for electrophysiology, containing either an mCherry or streptavidin tag, but no differences in function were observed. For expression analysis, enhanced GFP (EGFP)-tagged versions of full-length mouse *stoml1* cDNA, or a truncated version without the SCP2 domain (trSTOML1, amino acids 1–283), were amplified by high-fidelity DNA polymerase (Phusion® HF, New England Biolabs, Ipswich, MA, USA) and cloned into a pmEGFP-N3 vector (BD Biosciences Clontech, Palo Alto, CA, USA). The correct sequence was confirmed by full-length sequencing.

Immunocytochemistry

CHO cells were transfected with either STOML1-EGFP or trSTOML1-EGFP and imaged 24 h-hours after transfection using a Leica SP5 confocal microscope. For LysoTracker® Red (Life Technologies) labelling, DRG neurones transiently transfected 24 h prior to the experiment with either STOML1-EGFP or trSTOML1-EGFP were incubated at 37°C with 60 nM LysoTracker® Red in DRG growth medium (see above) for 1.5 h. Cells were subsequently washed with PBS and fixed with 4% paraformaldehyde for subsequent microscopic analysis using Leica LCS Lite and ImageJ.

Electrophysiology and data analysis

Whole-cell patch clamp recordings were conducted on DRG neurones and CHO cells at room temperature within 24 h of dissection/transfection, using the following solutions: extracellular (in mM) – NaCl (140), KCl (4), $CaCl_2$ (2), $MgCl_2$ (1), glucose (4), Hepes (10), adjusted to pH 7.4 with NaOH; intracellular – KCl (110), NaCl (10), $MgCl_2$ (1), EGTA (1) and Hepes (10), adjusted to pH 7.3 with KOH. Acidic extracellular solutions were made using either Hepes (pH 6.0) or MES (pH 5.0 and 4.0). Patch pipettes were pulled (P-97, Sutter Instruments, Novato, CA, USA) from borosilicate glass capillaries (Hilgenberg, Malsfeld, Germany) and had a resistance of 3–6 MΩ. Recordings were made using an EPC-9 amplifier (HEKA, Lambrecht/Pfalz, Germany) and Patchmaster© software (HEKA). Whole-cell currents were recorded at 20 kHz, pipette and membrane capacitance were compensated for using Patchmaster macros and series resistance was compensated by >60%. In DRG neurones, a standard voltage-step protocol was used whereby cells were held at

−120 mV for 150 ms before stepping to the test potential (−80 mV to +50 mV in 5 mV increments) for 40 ms, returning to the holding potential (−60 mV) for 200 ms between sweeps. Subsequently, cells were exposed to a 5 s pulse of pH 6.0, pH 5.0, pH 4.0 or 50 μM ATP applied in random order. Responses to acidic solutions were classified as transient, or sustained, based upon the initial response; for example, a rapidly inactivating transient current, followed by a sustained current during the acid application, was classified as a transient response. Cell diameter was measured by using MetaFluor (Molecular Devices, Sunnyvale, CA, USA), having used a stage micrometer to convert pixel values into micrometres.

For CHO cells, we stimulated cells with pH 6.0 and pH 4.0 solutions. Analysis was carried out using Fitmaster (HEKA) and GraphPad Prizm (GraphPad Software, Inc., La Jolla, CA, USA); current amplitudes were normalized to cell capacitance and values expressed as pA pF^{-1}.

Unpaired *t* tests or Mann–Whitney U tests were used to make comparisons between data sets to measure the effect of STOML1 coexpression in CHO cells and the lack of STOML1 in knockout mice compared to wild-type. Fisher's exact test was used to examine the comparative frequency of transient and sustained proton-gated currents in wild-type, compared to $STOML1^{-/-}$, neurones.

X-gal DRG neurone staining and analysis

Both thoracic and lumbar DRG were dissected out and placed into 0.5% glutaraldehyde in PBS on ice for 2 h. DRG were then washed several times in PBS and left in 30% sucrose overnight. DRG were subsequently embedded in Tissue-Tek OCT (Sakura) and 16 μm sections were cut on a cryostat CM300 (Leica) and mounted on slides for X-gal (5-bromo-4-chloro-3-indolyl-β-D-galactopyranoside) st aining. Sections were incubated in X-gal reaction buffer containing: 35 mM potassium ferrocyanide, 35 mM potassium ferricyanide, 2 mM $MgCl_2$ and 1 mg ml^{-1} X-gal, for 2 h at 37°C. Sections were subsequently washed in PBS until the solution no longer turned yellow and then observed on a Leica DM 5000B microscope using MetaVue software (Visitron, Puchheim, Germany). ImageJ was used to manually trace the outlines of cells in order to obtain cell area, which was then converted to diameter using Excel; histograms were plotted using GraphPad Prizm.

Results

Subcellular localisation of STOML1

In our hands no commercial or custom-made antibodies against STOML1 reliably and specifically detected endogenous STOML1 in either mouse DRG neurones or in cells lines transfected with STOML1. Therefore, we transfected both DRG neurones and CHO cells with mouse STOML1 cDNA constructs tagged with EGFP or the Strep-tag II (Korndorfer & Skerra, 2002). In agreement with a previous study using HeLa, MDCK and HepG2 cell lines (Mairhofer *et al.* 2009), we found that in both CHO cells and DRG neurones STOML1-EGFP is present within an intracellular pool of vesicles (Fig. 1*A* and *C*). However, we also observed STOML1-EGFP staining at the plasma membrane in CHO cells (Fig. 1*A*). In cultured DRG neurones transfected with STOML1-EGFP, STOML1 was seen to colocalise with the endosomal/lysosomal marker Lysotracker Red (Fig. 1*C*; Mairhofer *et al.* 2009). We also noted that STOML1-EGFP was present as puncta in DRG neurites that did not appear to colocalise with Lysotracker Red (Fig. 1*C*). These puncta may represent vesicles identical to those rich in stomatin and STOML3 that we have named transducosomes (Lapatsina *et al.* 2012*b*). To analyse the level of co-localisation of STOML1 with another member of the stomatin family, STOML3, DRG neurones were co-transfected with plasmids encoding fluorescently labelled proteins and the level of co-localisation was analysed. The level of STOML1 co-localisation with STOML3 was estimated to be around 70% with overlap coefficient: $r = 0.75$, SD = 0.18, SEM = 0.07, Pearson's coefficient: $r = 0.65$, data from six cells and three independent transfections, SD = 0.1, SEM = 0.04 (Supplementary Fig. 1).

STOML1 inhibits ASIC1a, but not its splice variant ASIC1b

We next investigated if co-expression with STOML1 affects the proton activation of ASIC subunits. We used CHO cells because they do not express endogenous, ASIC-like, proton-gated currents (Smith *et al.* 2007). In cells transfected with ASIC1a alone, stimulation with low pH solutions evoked transient inward currents (Fig. 2*A*, left panel), but in cells co-transfected with ASIC1a and STOML1 the amplitude of the peak response was almost completely ablated, with the reduction at pH 4.0 being over 90% (21.54 ± 3.09 pA pF^{-1}, $n = 34$, compared to 266.90 ± 44.42 pA pF^{-1}, $n = 42$, $P < 0.001$, Fig. 2*A* and *B*). This is the first observation of ASIC1a being modulated by a stomatin protein. STOML1 did not, however, affect the inactivation time constant of proton-gated ASIC1a currents (Fig. 2*C*). Whereas stomatin modulates ASIC3 and ASIC2a, no inhibitory effect was observed upon ASIC1a (Price *et al.* 2004) and we therefore sought to examine if the SCP2 domain, which is unique to STOML1 among stomatin family members, is required for ASIC1a modulation. We thus co-transfected CHO cells with ASIC1a and a truncated version of STOML1 (trSTOML1),

lacking amino acids 284–399, and observed that proton-gated currents were of similar appearance to those recorded from CHO cells transfected with ASIC1a alone: loss of the SCP2 domain resulted in a lack of ASIC1a inhibition by STOML1 (266.90 ± 44.42 pA pF^{-1}, $n = 42$ *vs.* 289.90 ± 98.28 pA pF^{-1}, $n = 12$ at pH 4.0, Fig. 2*A* right panel, *B* and *C*). One explanation for the lack of ASIC1a inhibition observed with trSTOML1 is that the protein is mislocalised. We therefore examined trSTOML1-EGFP expression in CHO cells and observed staining at the plasma membrane (Fig. 1*B*), similar to that seen with STOML1-EGFP (Fig. 1*A*), thus suggesting that trSTOML1 is processed normally by CHO cells. Moreover, in DRG neurones, trSTOML1-EGFP was observed as puncta in DRG neurone neurites just like STOML1-EGFP (Fig. 1*C* and *D*).

To further determine what structural domains of ASIC1a and STOML1 are required for the inhibition of ASIC1a, we recorded proton-gated currents from cells co-transfected with STOML1 and the ASIC1a splice variant ASIC1b. Unlike the inhibitory effect of STOML1 upon ASIC1a, no inhibition of proton-gated current was observed in cells co-transfected with ASIC1b and STOML1 (Fig. 2*D–F*).

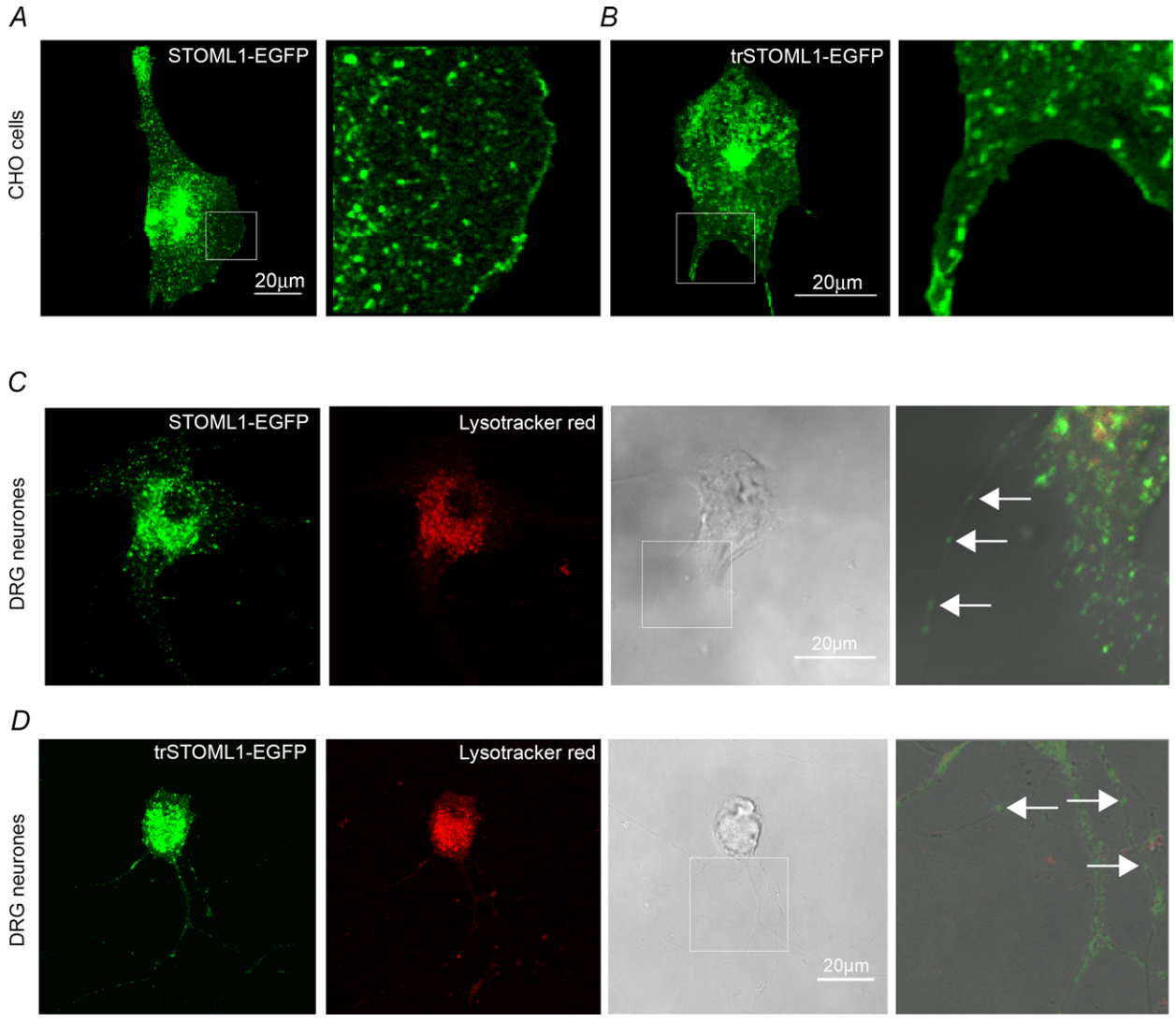

Figure 1. Localisation of STOML1-EGFP and trSTOML1-EGFP transiently expressed in CHO cells and DRG neurones
A and *B*, both STOML1-EGFP and trSTOML1-EGFP constructs display vesicular (left panels) and plasma membrane localisation, as seen at higher magnification (right panels showing area from white box in left panels). *C* and *D*, in cultured DRG neurones, STOML1-EGFP (*C*) and trSTOML1-EGFP (*D*) were observed in the intracellular vesicular pool, as well as in neurites as discrete puncta (see white arrows in far right panels displaying area from white box in phase contrast panel). The endosomal/lysosomal marker Lysotracker Red displayed a degree of co-localisation with STOML1 constructs, which was more predominant in the cell bodies.

STOML1 does not modulate ASIC2a

Like ASIC1, ASIC2 has two splice variants, but only ASIC2a forms functional, proton-gated homomers (Lingueglia *et al.* 1997). Whereas stomatin accelerates the inactivation time constant of ASIC2a (Price *et al.* 2004; Brand *et al.* 2012) and STOML3 inhibits current amplitude (Lapatsina *et al.* 2012*b*), STOML1 modulated neither ASIC2a proton-gated current amplitude nor inactivation time constant (Fig 3*A*–*C*).

STOML1 accelerates the ASIC3 inactivation time constant

Like ASIC2a, ASIC3 is modulated by both stomatin and STOML3, both of which cause inhibition of current amplitude (Price *et al.* 2004; Brand *et al.* 2012; Lapatsina *et al.* 2012*b*). In cells transfected with ASIC3 alone, proton-gated currents inactivated rapidly and at pH 4.0 the current did not fully inactivate within the 5 s application, resulting in a large sustained current, as we have observed

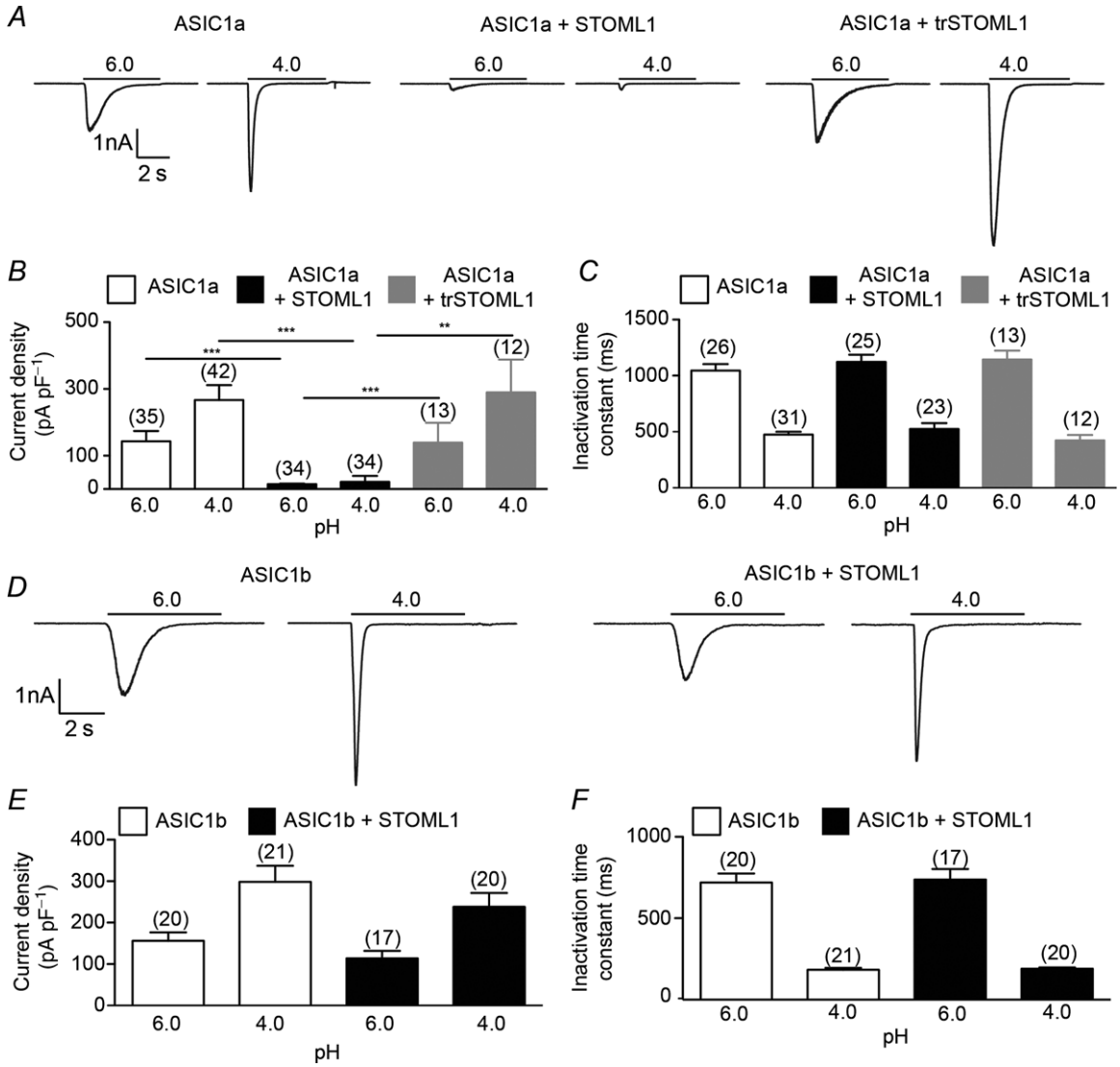

Figure 2. STOML1 inhibits ASIC1a, but not ASIC1b, in an SCP2 domain dependent mechanism
A, acid stimulation of cells expressing ASIC1a alone (left panel), ASIC1a and STOML1 (centre panel), or ASIC1a and trSTOML1 (right panel) showing that STOML-1 inhibits ASIC1a current amplitude in an SCP2 domain-dependent mechanism (data summarised in *B*). *C*, STOML1 has no modulatory effect upon the inactivation time constant of ASIC1a. *D*, acid stimulation of cells expressing ASIC1b alone (left panel) and ASIC1b and STOML1 (right panel) showing that ASIC1b current amplitude is not inhibited by STOML1 (data summarised in *E*). *F*, STOML1 has no modulatory effect upon the inactivation time constant of ASIC1b. Numbers in parentheses denote the number of cells recorded from. $^{**}P < 0.01$, $^{***}P < 0.001$.

previously (Brand *et al.* 2012). In cells co-transfected with ASIC3 and STOML1, no significant effect upon either the transient or the sustained current density was seen (Fig 3*D* and *E*), but the inactivation time constant was significantly faster at both pH 6.0 and pH 4.0 (Fig 3*F*).

STOML1 is expressed in approximately half of DRG neurones

We next focused on the role of STOML1 within the peripheral nervous system. The presence in the knockout animals of the betaGeo gene-trap cassette, which encodes a fusion protein of β-galactosidase, allowed us to study the promoter expression pattern of STOML1 in DRG neurones. DRGs were taken from lumbar/thoracic regions of STOML1$^{-/-}$ animals, and subjected to standard X-gal staining procedures. Positive X-gal cells constituted a substantial proportion of the DRG neurones with 748/1663 (44.98%) showing detectable X-gal staining (Fig 4*A*). Quantitative measurements of cell diameter showed that STOML1-positive neurones had significantly smaller mean diameters than STOML1-negative neurones (18.00 ± 0.18 μm *vs.* 22.42 ± 0.18 μm, $n = 748$ and 915, $P < 0.0001$, Fig 4*B*).

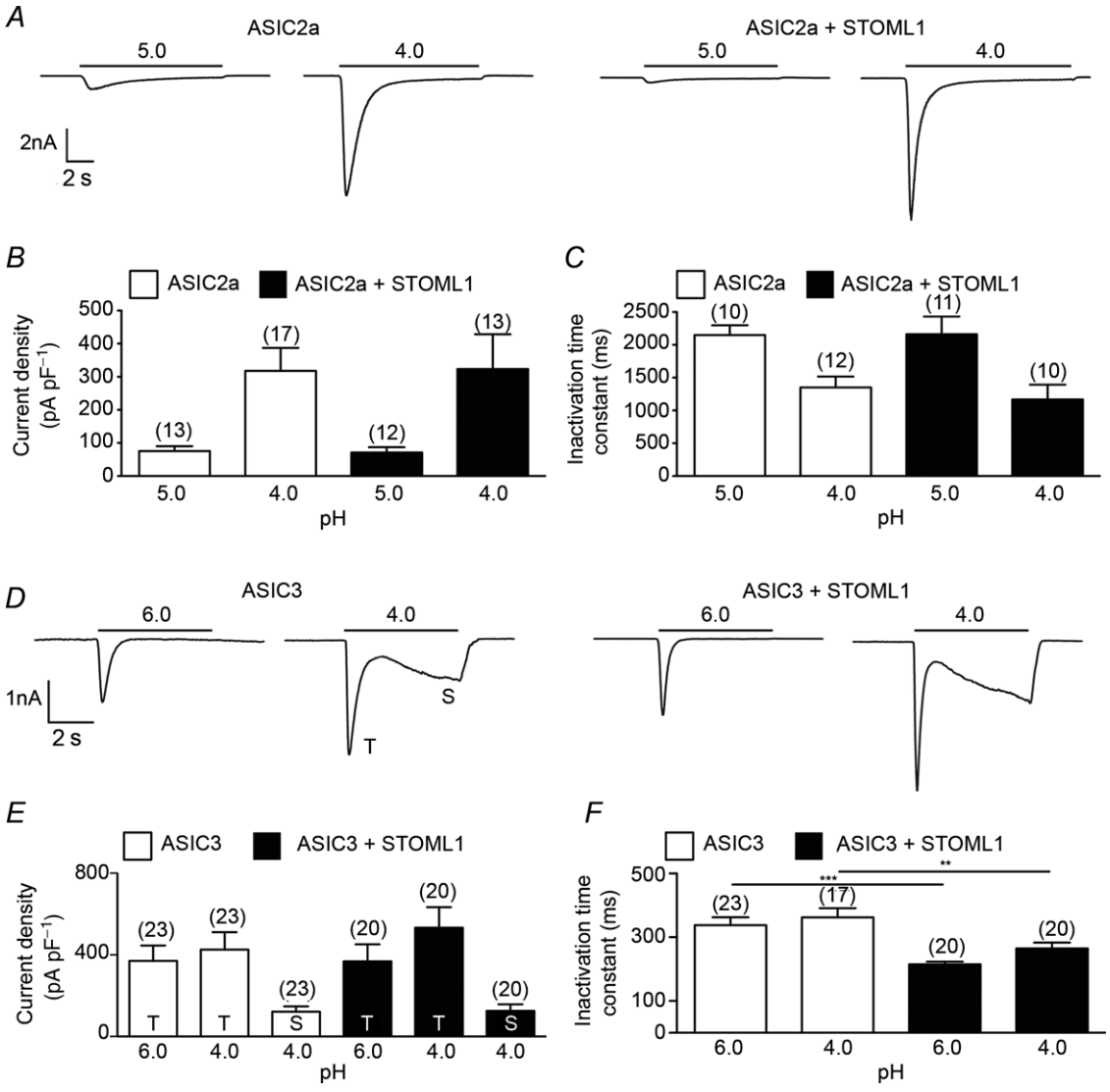

Figure 3. STOML1 has no effect upon ASIC2a, but accelerates the inactivation of ASIC3
A, acid stimulation of cells expressing ASIC2a alone (left panel) or ASIC1a and STOML1 (right panel) showing that ASIC2a is not inhibited by STOML1 (data summarised in *B*). *C*, STOML1 has no modulatory effect upon the inactivation time constant of ASIC2a. *D*, acid stimulation of cells expressing ASIC3 alone (left panel) or ASIC3 and STOML1 (right panel) showing that ASIC3 current amplitude is not inhibited by STOML1 (data summarised in *E*). *F*, STOML1 accelerates the inactivation time constant of ASIC3 at both pH 6.0 and pH 4.0. Numbers in parentheses denote the number of cells recorded from. $^{**}P < 0.01$, $^{***}P < 0.001$.

Using whole-cell electrophysiology, we next measured the properties of neurones from STOML1$^{-/-}$ mice compared to wild-type. In both wild-type and STOML1$^{-/-}$ DRG neurones we observed transient currents (T), which are probably mediated by ASICs, and sustained currents (S), which are probably mediated by a combination of transient receptor potential vanilloid 1 (TRPV1) activation and TWIK-related acid sensitive potassium (TASK) channel inhibition (Fig 4*C* and *D*; Smith *et al.* 2011). In both genotypes we observed that every cell demonstrated an inward current in response to acid stimulation. Across the pH range used (4.0–6.0), the frequency of T and S currents did not differ between genotypes, but in both genotypes there was a trend for T currents to be more prevalent at lower pH values (Fig 4*E*, details of cell diameters are given in Supplementary Table 1). When we assessed peak current amplitude, there was a trend at all pH values for currents

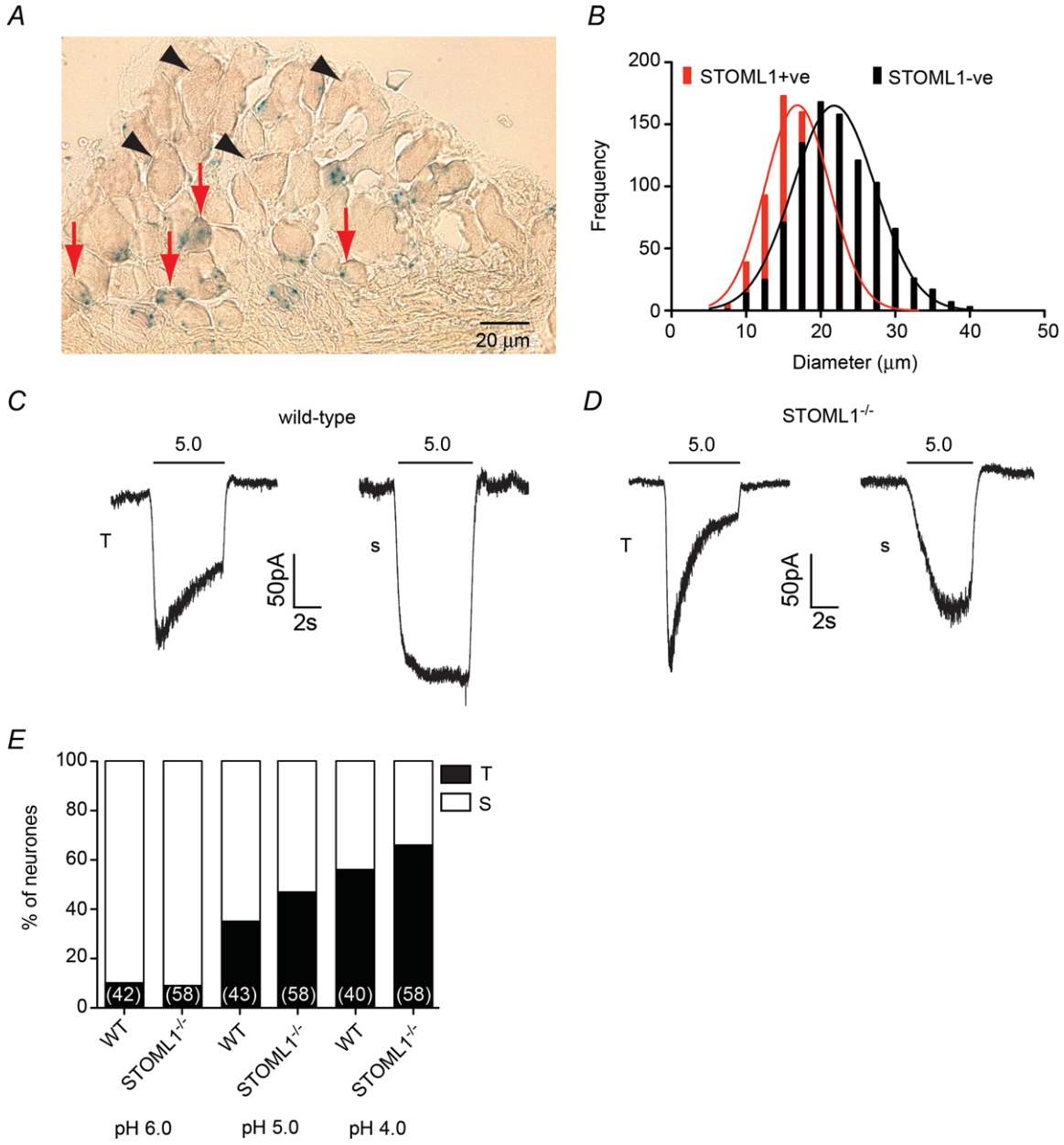

Figure 4. STOML1 is predominantly expressed in small diameter sensory neurones
A, thoracic DRG neurone section illustrating that X-gal staining, as a marker of STOML1, is largely present in small neurones (red arrows) and absent in large neurones (black arrowheads) (quantification in *B*). *C*, a pH 5.0 solution evokes both transient (T) and sustained (S) currents in wild-type neurones, as was also observed in neurones lacking STOML1 (*D*). *E*, percentage of transient responses increases as pH decreases in both genotypes. Numbers in parentheses denote the number of cells recorded from.

Table 1. Subunit-specific modulation of ASICs by stomatin family proteins. Different stomatin family members modulate specific ASIC subunits in different ways. '?' represents combinations that have not yet been examined; STOML2 and podocin have not yet been assessed and thus are absent from the table

	Stomatin	STOML1	STOML3
ASIC1a	No effect	Inhibits current amplitude	No effect
ASIC1b	?	No effect	?
ASIC2a	Increases inactivation speed	No effect	Inhibits current amplitude
ASIC2b		Homomers not activated by H^+	
ASIC3	Inhibits current amplitude	Increases inactivation speed	Inhibits current amplitude
ASIC4		Homomers not activated by H^+	

to be of greater magnitude in DRG neurones lacking STOML1, but this failed to reach significance (pH 6.0: wild-type 2.66 ± 0.39 pA pF^{-1}, $n = 42$ *vs.* STOML1$^{-/-}$ 3.86 ± 0.75 pA pF^{-1}, $n = 58$, $P = 0.099$; pH 5.0: wild-type 9.52 ± 1.70 pA pF^{-1}, $n = 43$ *vs.* STOML1$^{-/-}$ 14.13 ± 3.71 pA pF^{-1}, $n = 58$, $P = 0.315$; and pH 4.0: wild-type 26.46 ± 3.97 pA pF^{-1}, $n = 40$ *vs.* STOML1$^{-/-}$ 34.79 ± 4.30 pA pF^{-1}, $n = 58$, $P = 0.079$; Fig 5*A*).

Due to the different types of proton-gated currents present in DRG neurones and the observed inhibitory activity of STOML1 upon ASIC1a and ASIC3, we next examined the T and S proton-gated currents separately. For S currents, we observed significantly greater current amplitudes at pH 5.0 and pH 4.0 in STOML1$^{-/-}$ neurones compared to wild-type, but this was not true at pH 6.0 (Fig 5*B*). For T currents, currents were significantly larger at pH 6.0 in STOML1$^{-/-}$ neurones compared to wild-type, but there was no significant difference at lower pH (Fig 5*C*). In one set of experiments we also examined capsaicin sensitivity as a marker for functional TRPV1 channels, which can mediate sustained inward currents in response to protons (Smith *et al.* 2011). However, we found that only 8/14 and 3/16 pH 4.0 proton-gated sustained currents occurred in neurones that were also capsaicin sensitive in wild-type and STOML1$^{-/-}$ neurones, respectively, thus indicating that the sustained currents observed were not always necessarily mediated by TRPV1.

Considering that the modulation of ASIC3 by STOML1 decreases the inactivation time constant, we hypothesised that neurones lacking STOML1 may have slower inactivation time constants compared to those recorded in wild-type neurones. However, we found no evidence to support this hypothesis. Moreover, at pH 4.0, T currents actually inactivated more rapidly in neurones lacking STOML1 than in wild-type neurones (1243 ± 57 ms *vs.* 1596 ± 80 ms, $n = 31$ and 13, $P < 0.01$, Fig 5*D*).

Overall, these results are consistent with the hypothesis that lack of STOML1 will lead to a disinhibition of proton-gated currents in STOML1$^{-/-}$ neurones. Neither the magnitude of inward currents evoked by 50 μM ATP (Fig 5*E*) nor the amplitude of macroscopic voltage-gated inward currents were altered in neurones lacking STOML1 compared to wild-type neurones (Fig 5*F*).

Discussion

In this study we have shown that STOML1 largely resides in intracellular vesicles, but that a small proportion is present at the cell membrane where it modulates ASICs in a subunit-specific manner: ASIC1a and ASIC3 are modulated, but ASIC1b and ASIC2a are not. Using a STOML1$^{-/-}$ mouse, we show that STOML1 is expressed in approximately half of DRG neurones and that when proton-gated currents are split into transient and sustained groups, a lack of STOML1 is associated with significantly larger sustained proton-gated currents at very low pH and larger transient currents under moderately acidic conditions.

The stomatin family of proteins has been shown to interact with and modulate a variety of membrane protein transporters and ion channels (Lapatsina *et al.* 2012*a*). In this study have expanded the understanding of how stomatin domain family proteins modulate ASICs by characterising the effects of STOML1 on different ASIC subunits. Unlike stomatin, which has no inhibitory effect upon ASIC1a (Price *et al.* 2004), we observed a profound inhibition of proton-gated current amplitude in cells that were co-transfected with ASIC1a and STOML1 compared to cells that were transfected with ASIC1a alone. We further demonstrated that specific structural elements of both ASIC1a and STOML1 are required for inhibition to occur: the splice variant of ASIC1a, ASIC1b, is not inhibited by STOML1 and a truncated version of STOML1 lacking the SCP2 domain was unable to modulate ASIC1a. The alternative splice variants of ASIC1 result in proteins that differ from the intracellular N termini until approximately one-third of the way through the extracellular loop (Bassler *et al.* 2001). The typical structure of stomatin family proteins suggests that STOML1 is likely to be anchored into the plasma membrane with both N and C termini of the protein being intracellular (Lapatsina *et al.* 2012*a*), and therefore the most likely site of interaction between STOML1 and

ASIC1a is the intracellular N terminus, which is different in ASIC1b and may thus result in a lack of modulation. The loss of the SCP2 domain in STOML1 also resulted in a lack of ASIC1a inhibition, suggesting that the SCP2 domain may be directly involved in the interaction with ASIC1a; our demonstration that trSTOML1-EGFP displays similar cell membrane staining to STOML1-EGFP rules out the possibility of substantial mislocalisation of the truncated form of the protein. A further possibility is that STOML1 oligomerisation is required for inhibition of ASIC1a, as we have shown for the inhibitory effect of stomatin upon ASIC3 (Brand *et al.* 2012), and that the SCP2 domain is needed for oligomerisation of STOML1 proteins. Future studies will be focused on gaining a better understanding of the structural prerequisites for functional modulation of ASIC1a by STOML1.

Unlike ASIC1a, STOML1 exerted no inhibitory action upon ASIC2a-mediated proton-gated currents. Cells transfected with STOML1 and ASIC3 displayed proton-gated currents that inactivated significantly more rapidly than in cells transfected with ASIC3 alone, but current amplitude was not affected. This result is similar to that of stomatin upon ASIC2a where the current inactivation time constant is accelerated with no effect

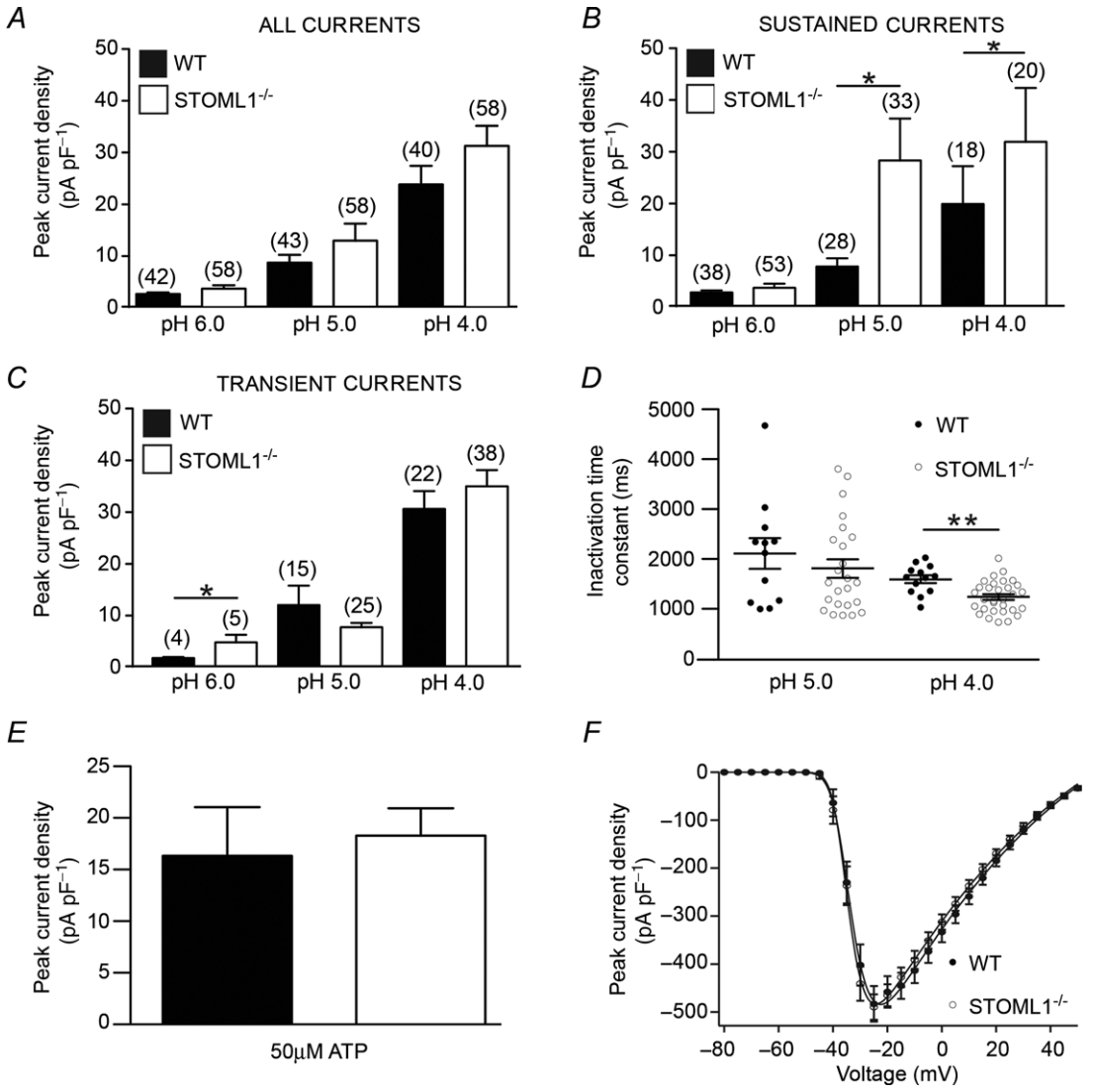

Figure 5. Loss of STOML1 leads to disinhibition of some proton-gated currents in DRG neurones
A, at all pHs tested, peak proton-gated current magnitude was larger in DRG neurones lacking STOML1, but this failed to reach significance. *B*, sustained currents are significantly greater at pH 5.0 and 4.0, but not at pH 6.0 in STOML1$^{-/-}$ DRG neurones. *C*, transient currents are significantly greater at pH 6.0, but not at lower values in STOML1$^{-/-}$ DRG neurones. *D*, transient currents in STOML1$^{-/-}$ DRG neurones inactivated significantly more rapidly at pH 4.0, but not at pH 5.0. No significant differences were observed in the magnitude of either ATP-activated (*E*) or voltage-gated (*F*) inward currents. *$P < 0.05$, **$P < 0.01$. Numbers in parentheses denote the number of recorded cells.

upon current amplitude (Price *et al.* 2004; Brand *et al.* 2012). Overall, these results add to the growing understanding of how ASICs are modulated by different members of the stomatin family, as summarised in Table 1.

Our observation that STOML1 modulates both ASIC1a and ASIC3 prompted us to identify changes in DRG neurone proton-gated currents in mice that lack STOML1. Staining for X-gal in STOML1 knockout mice showed that STOML1 is present in almost half of DRG neurones and that these neurones are significantly smaller than neurones lacking STOML1, but there is a considerable overlap in the diameters of STOML1-positive and STOML1-negative neurones.

In our electrophysiology studies, we observed an increased prevalence of transient currents in neurones from both genotypes as the pH decreased, which may reflect the fact that ASIC2-containing ASIC heteromers are predominant in mouse DRG neurones because ASIC2-containing heteromers are less pH sensitive than ASIC1/3 channels and do not produce large transient currents until below pH 5.0 (Babinski *et al.* 2000; Hesselager *et al.* 2004; Smith *et al.* 2007). Based upon our studies with STOML1 and ASICs in CHO cells, one might expect to observe larger proton-gated currents due to a lack of inhibition of ASIC1a, as well as more slowly inactivating currents due a lack of modulation of ASIC3. However, in mouse DRG neurones, there is no convincing evidence for a subset of neurones expressing homomeric ASIC1a; indeed ASIC-like currents are most likely mediated by heteromeric ASICs (Benson *et al.* 2002). Even in rat DRG neurones, where a subset of DRG neurones has been identified to express only ASIC1a-mediated proton-gated currents, these neurones have been estimated to make up less than 5% of the total population (Deval *et al.* 2008). Although there was a trend for proton-gated currents to be larger in STOML1$^{-/-}$ neurones, this did not reach significance at any pH. However, when we analysed the data in more detail and split currents into transient (ASIC-like) and sustained (non-ASIC-like), we did observe some significant differences: sustained currents were significantly larger in STOML$^{-/-}$ neurones at the lowest pH tested and transient currents were significantly larger in STOML$^{-/-}$ neurones at pH 6.0. The larger sustained currents at lower pH may seem confusing considering that we only observed inhibition of current amplitude in cells expressing ASIC1a, which produces a transient current in response to protons. However, the identity of many of the sustained currents that we recorded remains unknown. A key candidate for mediating sustained currents is the capsaicin-gated ion channel TRPV1, although in both wild-type and STOML1$^{-/-}$ small neurones we observed sustained currents in the absence of capsaicin sensitivity; proton-gated sustained currents in capsaicin-insensitive rat DRG neurones that are also not inhibited by the TRPV1 antagonist capsazepine have been previously reported (Liu *et al.* 2004). Furthermore, in both mouse and naked mole-rat we have previously shown that approximately half of DRG neurones that exhibit a sustained response to protons do so in a TRPV1-independent manner, as demonstrated by a failure of the TRPV1 antagonist BCTC (4-(3-Chloro-2-pyridinyl)-N-[4-(1,1-dimethylethyl)phenyl]-1-piperazinecarboxamide) to inhibit the current and capsaicin-insensitivity (Smith *et al.* 2011). Sustained currents could also be the result of TASK channel inhibition, but there is also good reason to think that ASIC subunits could contribute to sustained currents. For example, STOML3 inhibits ASICs, which mediate largely transient currents, and yet proton-gated sustained currents, which were blocked by the ASIC antagonist amiloride, were observed to be larger in neurones that lack ASIC3 (Wetzel *et al.* 2007), similar to the result observed here in STOML1 mutant neurones. The disinhibition of certain proton-gated currents in STOML1$^{-/-}$ neurones appeared specific because neither inward currents mediated by ATP nor voltage were significantly different between genotypes.

In conclusion, we have shown that STOML1 modulates ASICs in a subunit-specific manner and that DRG neurones lacking STOML1 do have larger proton-gated currents at some pH values. The relatively mild, yet specific, disinhibition observed in STOML1$^{-/-}$ neurones suggests that ASIC1a and/or ASIC1a-containing heteromers contribute to proton sensing in DRG neurones and thus we have identified a novel modulator of ASIC1a channels; future investigations will concentrate on the implications of STOML1 modulation of ASIC1a in the central nervous system where ASIC1a plays a role in many physiological and pathophysiological states (Wemmie *et al.* 2013).

References

Babinski K, Catarsi S, Biagini G & Seguela P (2000). Mammalian ASIC2a and ASIC3 subunits co-assemble into heteromeric proton-gated channels sensitive to Gd^{3+}. *J Biol Chem* **275**, 28519–28525.

Barnes TM, Jin Y, Horvitz HR, Ruvkun G & Hekimi S (1996). The *Caenorhabditis elegans* behavioral gene *unc-24* encodes a novel bipartite protein similar to both erythrocyte band 7.2 (stomatin) and nonspecific lipid transfer protein. *J Neurochem* **67**, 46–57.

Bassler EL, Ngo-Anh TJ, Geisler HS, Ruppersberg JP & Grunder S (2001). Molecular and functional characterization of acid-sensing ion channel (ASIC) 1b. *J Biol Chem* **276**, 33782–33787.

Benson CJ, Xie J, Wemmie JA, Price MP, Henss JM, Welsh MJ & Snyder PM (2002). Heteromultimers of DEG/ENaC subunits form H^+-gated channels in mouse sensory neurons. *Proc Natl Acad Sci U S A* **99**, 2338–2343.

Brand J, Smith ESJ, Schwefel D, Lapatsina L, Poole K, Omerbašić D, Kozlenkov A, Behlke J, Lewin GR & Daumke O (2012). A stomatin dimer modulates the activity of acid-sensing ion channels. *EMBO J* **31**, 3635–3646.

Cadiou H, Studer M, Jones NG, Smith ES, Ballard A, McMahon SB & McNaughton PA (2007). Modulation of acid-sensing ion channel activity by nitric oxide. *J Neurosci* **27**, 13251–13260.

Deval E, Noel J, Lay N, Alloui A, Diochot S, Friend V, Jodar M, Lazdunski M & Lingueglia E (2008). ASIC3, a sensor of acidic and primary inflammatory pain. *EMBO J* **27**, 3047–3055.

Diochot S, Baron A, Salinas M, Douguet D, Scarzello S, Dabert-Gay A-S, Debayle D, Friend V, Alloui A, Lazdunski M & Lingueglia E (2012). Black mamba venom peptides target acid-sensing ion channels to abolish pain. *Nature* **490**, 552–555.

Gallagher PG & Forget BG (1995). Structure, organization, and expression of the human band 7.2b gene, a candidate gene for hereditary hydrocytosis. *J Biol Chem* **270**, 26358–26363.

Goodman MB, Ernstrom GG, Chelur DS, O'Hagan R, Yao CA & Chalfie M (2002). MEC-2 regulates *C. elegans* DEG/ENaC channels needed for mechanosensation. *Nature* **415**, 1039–1042.

Hesselager M, Timmermann DB & Ahring PK (2004). pH dependency and desensitization kinetics of heterologously expressed combinations of acid-sensing ion channel subunits. *J Biol Chem* **279**, 11006–11015.

Jones RC, Xu L & Gebhart GF (2005). The mechanosensitivity of mouse colon afferent fibers and their sensitization by inflammatory mediators require transient receptor potential vanilloid 1 and acid-sensing ion channel 3. *J Neurosci* **25**, 10981–10989.

Kellenberger S & Schild L (2002). Epithelial sodium channel/degenerin family of ion channels: a variety of functions for a shared structure. *Physiol Rev* **82**, 735–767.

Korndorfer IP & Skerra A (2002). Improved affinity of engineered streptavidin for the Strep-tag II peptide is due to a fixed open conformation of the lid-like loop at the binding site. *Protein Sci* **11**, 883–893.

Lapatsina L, Brand J, Poole K, Daumke O & Lewin GR (2012*a*). Stomatin-domain proteins. *Eur J Cell Biol* **91**, 240–245.

Lapatsina L, Jira JA, Smith ESJ, Poole K, Kozlenkov A, Bilbao D, Lewin GR & Heppenstall PA (2012*b*). Regulation of ASIC channels by a stomatin/STOML3 complex located in a mobile vesicle pool in sensory neurons. *Open Biol* **2**, 120096, DOI: 10.1098/rsob.120096.

Lingueglia E, de Weille JR, Bassilana F, Heurteaux C, Sakai H, Waldmann R & Lazdunski M (1997). A modulatory subunit of acid sensing ion channels in brain and dorsal root ganglion cells. *J Biol Chem* **272**, 29778–29783.

Liu M, Willmott NJ, Michael GJ & Priestley JV (2004). Differential pH and capsaicin responses of *Griffonia simplicifolia* IB4 (IB4)-positive and IB4-negative small sensory neurons. *Neuroscience* **127**, 659–672.

Mairhofer M, Steiner M, Salzer U & Prohaska R (2009). Stomatin-like protein-1 interacts with stomatin and is targeted to late endosomes. *J Biol Chem* **284**, 29218–29229.

Martinez-Salgado C, Benckendorff AG, Chiang L-Y, Wang R, Milenkovic N, Wetzel C, Hu J, Stucky CL, Parra MG, Mohandas N & Lewin GR (2007). Stomatin and sensory neuron mechanotransduction. *J Neurophysiol* **98**, 3802–3808.

Mazzuca M, Heurteaux C, Alloui A, Diochot S, Baron A, Voilley N, Blondeau N, Escoubas P, Gélot A, Cupo A, Zimmer A, Zimmer AM, Eschalier A & Lazdunski M (2007). A tarantula peptide against pain via ASIC1a channels and opioid mechanisms. *Nat Neurosci* **10**, 943–945.

Moshourab RA, Wetzel C, Martinez-Salgado C & Lewin GR (2013). Stomatin-domain protein interactions with acid sensing ion channels modulate nociceptor mechanosensitivity. *J Physiol* **591**, 5555–5574.

O'Hagan R, Chalfie M & Goodman MB (2005). The MEC-4 DEG/ENaC channel of *Caenorhabditis elegans* touch receptor neurons transduces mechanical signals. *Nat Neurosci* **8**, 43–50.

Page AJ, Brierley SM, Martin CM, Martinez-Salgado C, Wemmie JA, Brennan TJ, Symonds E, Omari T, Lewin GR, Welsh MJ & Blackshaw LA (2004). The ion channel ASIC1 contributes to visceral but not cutaneous mechanoreceptor function. *Gastroenterology* **127**, 1739–1747.

Price MP, Lewin GR, McIlwrath SL, Cheng C, Xie J, Heppenstall PA, Stucky CL, Mannsfeldt AG, Brennan TJ, Drummond HA, Qiao J, Benson CJ, Tarr DE, Hrstka RF, Yang B, Williamson RA & Welsh MJ (2000). The mammalian sodium channel BNC1 is required for normal touch sensation. *Nature* **407**, 1007–1011.

Price MP, McIlwrath SL, Xie J, Cheng C, Qiao J, Tarr DE, Sluka KA, Brennan TJ, Lewin GR & Welsh MJ (2001). The DRASIC cation channel contributes to the detection of cutaneous touch and acid stimuli in mice. *Neuron* **32**, 1071–1083.

Price MP, Thompson RJ, Eshcol JO, Wemmie JA & Benson CJ (2004). Stomatin modulates gating of acid-sensing ion channels. *J Biol Chem* **279**, 53886–53891.

Rungaldier S, Oberwagner W, Salzer U, Csaszar E & Prohaska R (2013). Stomatin interacts with GLUT1/SLC2A1, band 3/SLC4A1, and aquaporin-1 in human erythrocyte membrane domains. *Biochim Biophys Acta* **1828**, 956–966.

Seidel G & Prohaska R (1998). Molecular cloning of hSLP-1, a novel human brain-specific member of the band 7/MEC-2 family similar to *Caenorhabditis elegans* UNC-24. *Gene* **225**, 23–29.

Sherwood TW, Frey EN & Askwith CC (2012). Structure and activity of the acid-sensing ion channels. *Am J Physiol Cell Physiol* **303**, C699–C710.

Smith ES & Lewin GR (2009). Nociceptors: a phylogenetic view. *J Comp Physiol A* **195**, 1089–1106.

Smith ES, Zhang X, Cadiou H & McNaughton PA (2007). Proton binding sites involved in the activation of acid-sensing ion channel ASIC2a. *Neurosci Lett* **426**, 12–17.

Smith ESJ, Omerbašić D, Lechner SG, Anirudhan G, Lapatsina L & Lewin GR (2011). The molecular basis of acid insensitivity in the African naked mole-rat. *Science* **334**, 1557–1560.

Stewart GW, Hepworth-Jones BE, Keen JN, Dash BC, Argent AC & Casimir CM (1992). Isolation of cDNA coding for an ubiquitous membrane protein deficient in high Na^+, low K^+ stomatocytic erythrocytes. *Blood* **79**, 1593–1601.

Tavernarakis N, Driscoll M & Kyrpides NC (1999). The SPFH domain: implicated in regulating targeted protein turnover in stomatins and other membrane-associated proteins. *Trends Biochem Sci* **24**, 425–427.

Wemmie JA, Chen J, Askwith CC, Hruska-Hageman AM, Price MP, Nolan BC, Yoder PG, Lamani E, Hoshi T, Freeman JH & Welsh MJ (2002). The acid-activated ion channel ASIC contributes to synaptic plasticity, learning, and memory. *Neuron* **34**, 463–477.

Wemmie JA, Taugher RJ & Kreple CJ (2013). Acid-sensing ion channels in pain and disease. *Nat Rev Neurosci* **14**, 461–471.

Wetzel C, Hu J, Riethmacher D, Benckendorff A, Harder L, Eilers A, Moshourab R, Kozlenkov A, Labuz D, Caspani O, Erdmann B, Machelska H, Heppenstall PA & Lewin GR (2007). A stomatin-domain protein essential for touch sensation in the mouse. *Nature* **445**, 206–209.

Xiong ZG, Zhu XM, Chu XP, Minami M, Hey J, Wei WL, MacDonald JF, Wemmie JA, Price MP, Welsh MJ & Simon RP (2004). Neuroprotection in ischemia: blocking calcium-permeable acid-sensing ion channels. *Cell* **118**, 687–698.

Yokoyama H, Fujii S & Matsui I (2008). Crystal structure of a core domain of stomatin from pyrococcus horikoshii illustrates a novel trimeric and coiled-coil fold. *J Mol Biol* **376**, 868–878.

Zhan H, Moore CS, Chen B, Zhou X, Ma X-M, Ijichi K, Bennett MVL, Li X-J, Crocker SJ & Wang Z-W (2012). Stomatin inhibits pannexin-1-mediated whole-cell currents by interacting with its carboxyl terminal. *PLoS ONE* **7**, e39489.

Zhang J-Z, Abbud W, Prohaska R & Ismail-Beigi F (2001). Overexpression of stomatin depresses GLUT-1 glucose transporter activity. *Am J Physiol Cell Physiol* **280**, C1277–C1283.

Ziemann AE, Allen JE, Dahdaleh NS, Drebot II, Coryell MW, Wunsch AM, Lynch CM, Faraci FM, Howard MA, Welsh MJ & Wemmie JA (2009). The amygdala is a chemosensor that detects carbon dioxide and acidosis to elicit fear behavior. *Cell* **139**, 1012–1021.

Ziemann AE, Schnizler MK, Albert GW, Severson MA, Howard MA, Welsh MJ & Wemmie JA (2008). Seizure termination by acidosis depends on ASIC1a. *Nat Neurosci* **11**, 816–822.

Additional information

Competing interests

None declared.

Author contributions

A.K., L.L., G.R.L. and E.S.S. were responsible for the collection, analysis and interpretation of data. A.K., G.R.L. and E.S.S. drafted the article. A.K., G.R.L. and E.S.S. designed the experiments. All authors have read and approved the final version of the manuscript.

Funding

This project was supported by grants of the German Research Council (SFB449/B18 and SFB958/A09 to G.R.L.).

Acknowledgements

We thank H. Thränhardt for technical assistance. Experiments were carried out at the MDC, analysis was carried out at the MDC and at the University of Cambridge.